ANTIOXIDANTS & REDOX SIGNALING
Volume 10, Number 1, 2008

DOI: 10.1089/ars.2007.1837

Forum Original Research Communication

In Vivo Reduction-Oxidation State of Protein Disulfide Isomerase: The Two Active Sites Independently Occur in the Reduced and Oxidized Forms

CHRISTIAN APPENZELLER-HERZOG[1,2] and LARS ELLGAARD[1,2]

ABSTRACT

Thiol-disulfide oxidoreductases of the human protein disulfide isomerase (PDI) family promote protein folding in the endoplasmic reticulum (ER), while also assisting the retrotranslocation of toxins and misfolded ER proteins to the cytosol. The redox activity of PDI-like proteins is determined by the redox state of active-site cysteines found in a Cys-Xaa-Xaa-Cys motif. Progress in understanding redox regulation of the mammalian enzymes is currently hampered by the lack of reliable methods to determine quantitatively their redox state in living cells. We developed such a method based on the alkylation of cysteines by methoxy polyethylene glycol 5000 maleimide. With this method, we showed for the first time that *in vivo* PDI is present in two semi-oxidized forms in which either the first active site (in the a domain) or the second active site (in the a′ domain) is oxidized. We report a steady-state redox distribution of endogenous PDI in HEK-293 cells of 50 ± 5% fully reduced, 18 ± 2% a-oxidized/a′-reduced, 15 ± 2% a-reduced/a′-oxidized, and 16 ± 4% fully oxidized. These results suggest that neither of the two domains in human PDI exclusively catalyzes substrate oxidation or reduction *in vivo*. *Antioxid. Redox Signal.* 10, 55–64.

INTRODUCTION

The formation of disulfide bonds in newly synthesized proteins in the endoplasmic reticulum (ER) involves the oxidation of thiols and the reduction and isomerization of nonproductive disulfides (9). These processes are catalyzed by thiol-disulfide oxidoreductases such as protein disulfide isomerase (PDI; EC 5.3.4.1). PDI comprises two active-site domains (**a** and **a′**; Fig. 1B), each with a Cys-Gly-His-Cys sequence motif that facilitates the transfer of disulfide bonds by forming a short-lived, covalent reaction intermediate with cysteines in substrate proteins. Recent *in vitro* work on *Saccharomyces cerevisiae* PDI (Pdi1p) suggests intramolecular domain cooperation, so that catalysis of substrate oxidation is performed primarily by the **a′** domain, whereas disulfide isomerization reactions are facilitated by the **a** domain (18, 32). Catalysis of dithiol oxidation requires the active-site cysteines in the oxidized form, whereas they must be reduced to catalyze disulfide-bond reduction. Thus, the *in vivo* reduction–oxidation (redox) state of the two active sites in PDI is fundamental for determining its biologic function.

A number of methods have been used to determine the *in vivo* redox state for enzymes of the human PDI family that to date counts 17 published members (9). In a crucial first step, care is taken to prevent thiol-disulfide exchange reactions from taking place during and after cell lysis. This problem is most commonly solved by incubating cells in a buffer containing cell-permeable, thiol-reactive alkylating reagents such as *N*-ethylmaleimide (NEM) or in acid to protonate the reactive thiolate anions. In subsequent steps, active-site cysteines are modified by various reagents so as to create a difference between free cysteines and those present in disulfide bonds. For instance, in the particularly useful protocol recently developed by the Bulleid laboratory (16), cells are first subjected to *in situ* mod-

[1]Institute of Biochemistry, Swiss Federal Institute of Technology (ETH), ETH-Hoenggerberg, Zurich, Switzerland.
[2]Current address: Department of Molecular Biology, University of Copenhagen, Copenhagen, Denmark.

ification with NEM (125 Da) to block free cysteines. After cell lysis, disulfides are broken by the reducing agent Tris(2-carboxyethyl)phosphine (TCEP) and then alkylated by 4-acetamido-4′-maleimidylstilbene-2,2′-disulfonic acid (AMS; 536 Da). As a result of the size difference between NEM and AMS, oxidized proteins run slower by SDS-PAGE after modification. A step-by-step overview of this method and the newly developed methods used here is provided in Fig. 1A.

Previous efforts to separate the different redox forms present *in vivo* of human PDI by native PAGE (20, 23) or by SDS-PAGE after alkylation of active-site cysteines with AMS (5, 20, 21, 24) have yielded results that were difficult to interpret and

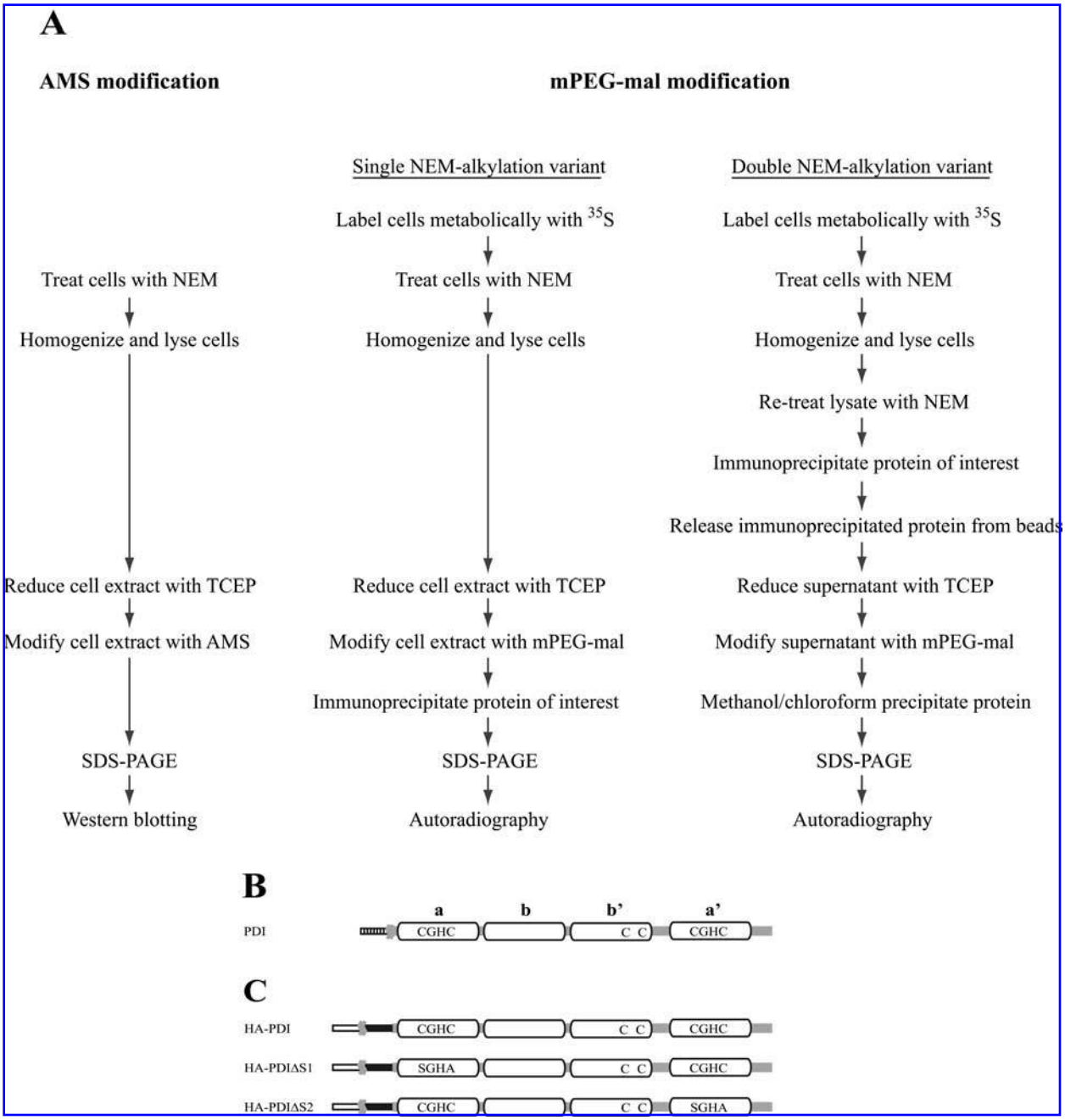

FIG. 1. Graphic overview of the methods and proteins used in this study. (**A**) Outline of the AMS and mPEG-mal modification procedures. (**B**) Human PDI is composed of four thioredoxin-like domains: **a**, **b**, **b′**, and **a′** (*white boxes*). The catalytic domains, **a** and **a′**, each contain a Cys-Gly-His-Cys (CGHC) active-site motif. The two noncatalytic cysteine residues in the **b′** domain that are known not to form a disulfide also are shown. The *dashed bar* at the N-terminus represents the signal sequence, and the signal peptidase-cleavage site is indicated by the *grey zig-zag lines*. (**C**) Recombinant wild-type and mutant PDI constructs. The signal sequence of ERp44 (*white bar*) is followed directly by an HA epitope (*black bar*). In HA-PDIΔS1 and HA-PDIΔS2, the two active-site cysteines in the **a** or the **a′** domain, respectively, were changed to serine (S) and alanine (A).

not possible to quantify reliably. Here, we describe a method to determine the *in vivo* redox state of human PDI that is based on the alkylation of cysteines by methoxy polyethylene glycol 5000 maleimide (mPEG-mal), a reagent previously used to investigate the redox state of the protein *in vitro* (30). We show that the method provides a very clear separation of oxidized and reduced PDI that allows the reliable quantification of each species. We demonstrate for the first time the presence of two semioxidized forms of PDI and map the molecular identity of each of them to redox states with the **a** domain oxidized and the **a′** domain reduced, and *vice versa*. The biologic implications of this finding are discussed, along with the potential for using the method to establish the *in vivo* redox state of virtually any protein containing structural disulfides.

MATERIALS AND METHODS

Reagents

NEM, TCEP (stock 0.2 *M*, 50 m*M* Tris/NaOH pH 7, stored at −20°C), dithiothreitol (DTT, stock 1 *M*, H_2O, stored at −20°C), and diamide (stock 0.5 *M*, H_2O, stored at −20°C), were from Sigma Chemical Co. (St. Louis, MO). mPEG-mal (stock 55 m*M*, dimethyl sulfoxide, stored at −80°C and melted at 30°C just before use) was from Nektar Therapeutics (Huntsville, AL). AMS (stock 75 m*M*, dimethyl sulfoxide, stored at −20°C) was purchased from Invitrogen (Carlsbad, CA). Promix L[^{35}S] *in vitro* cell-labeling mix and protein A-sepharose were from GE Healthcare (Piscataway, NJ). A polyclonal rabbit antiserum against PDI (SPA-890), used for immunoprecipitation and Western blotting, was obtained from Stressgen (Victoria, BC, Canada). The HA.11 mouse monoclonal antibody (clone 16B12) was purchased from Covance Research Products (Berkeley, CA), and our affinity-purified rabbit antiserum specific for thioredoxin-related transmembrane protein 3 (TMX3) has previously been described (15).

Recombinant DNA constructs

To obtain pcDNA3/HA-PDI, pcDNA3/HA-PDIΔS1, and pcDNA3/HA-PDIΔS2, we amplified the region encoding mature PDI (after signal peptide cleavage) from wtPDI, PDIΔS1 (C36S, C39A) and PDIΔS2 (C380S, C383A) [(7), a kind gift from Jakob R. Winther] by PCR by using 5′-CATGGTACCGACGCCCCCGAGGAGG-3′ as forward primer and 5′-CATTCTAGATTACAGTTCATCTTTCACAGC-3′ as reverse primer. The resulting PCR fragments featuring an in-frame KpnI-site at the 5′-end and an XbaI-site at the 3′-end (both underlined) were cloned into a derivative of the mammalian expression vector pcDNA3. This construct encoded the ERp44 signal sequence followed by an HA epitope tag and an in-frame KpnI site, and was generated by inserting a HindIII/XhoI fragment comprising the ERp44ss-HA-KpnI cassette derived from pcDNA3.1-ERp57-HA [(25), kindly provided by Roberto Sitia] into pcDNA3. The mature protein products after cleavage of the ERp44 signal sequence contain an N-terminal HA-tag followed by the three additional amino acids, Glu-Gly-Thr, and finally the PDI sequences (see Fig. 1C). The correct sequence of all constructs was confirmed by DNA sequencing.

Cell culture, transfection, metabolic labeling, and drug treatment

HEK-293 (Human Embryonic Kidney 293) cells (ATCC CRC-1573) and Vero cells (ATCC CCL-81) were maintained in α-minimal essential medium (Invitrogen), supplemented with 10 % (vol/vol) fetal calf serum at 37°C under 5% CO_2. Foreign DNA was introduced into HEK-293 cells by using Lipofectamine 2000 (Invitrogen), according to the manufacturer's protocol. For metabolic labeling, cells were incubated overnight at 37°C in Dulbecco's modified Eagle's medium without methionine and cystine (Sigma), supplemented with 2% fetal calf serum and 100 μCi of pro-mix L[^{35}S].

DTT and diamide treatment, in situ NEM-alkylation, cell homogenization, and lysis

Treatment of cells with 10 m*M* DTT or 5 m*M* diamide was performed for 5 min at 37°C in full growth medium. To block the sulfhydryl groups of free cysteines *in situ,* cell monolayers were washed with ice-cold phosphate-buffered saline (PBS; 154 m*M* NaCl, 1.9 m*M* KH_2PO_4, 8.1 m*M* Na_2HPO_4, pH 7.3) containing 20 m*M* NEM, and incubated in the same buffer on ice for 20 min. The cells were then scraped from the culture dish by using a rubber policeman in 1 ml 80 m*M* Tris/HCl pH 7.0, 200 μ*M* PMSF, pelleted in a microfuge tube for 1 min at 20,000 *g* at 4°C, and the pellets homogenized in 100 μl of the same buffer by 10 passages through a 25-G needle. After addition of 10 μl of 10% SDS, the samples were denatured for 10 min in a heat block at 97°C.

AMS modification protocol

The protocol originally developed by Jessop and co-workers (16) was used. In brief, cells grown in six-well plates (Nunc, Roskilde, Denmark) were subjected to *in situ* NEM-alkylation, homogenized, and lysed in buffer containing SDS. For each lane subsequently loaded on a gel and analyzed with Western blotting, 10 μl of this lysate was reduced for 15 min by the addition of 0.5 μl of 200 m*M* TCEP and alkylated for 1 h by addition of 2.5 μl of 75 m*M* AMS.

PEG-mal modification protocols

In the single NEM-alkylation variant, HEK-293 cells were grown and metabolically labeled overnight in six-well plates, subjected to *in situ* NEM-alkylation, homogenized in 50 μl of 80 m*M* Tris/HCl, pH 7.0, 200 μ*M* PMSF, and lysed by addition of 5 μl 10% SDS at 97°C. Then 40 μl of the lysate was reduced for 15 min by addition of 2 μl of 200 m*M* TCEP and alkylated for 1 h by addition of 15 μl of 55 m*M* mPEG-mal. By the subsequent immunoprecipitation of PDI or TMX3, excess mPEG-mal was removed ahead of SDS-PAGE and phosphorimaging (see later).

In the double NEM-alkylation variant, ^{35}S-labeled and NEM-modified cell lysates were produced as described earlier (homogenization volume, 100 μl) and denatured for 60 min at 97°C with occasional vortexing. Extensive heat denaturation ahead of the second alkylation with NEM proved beneficial for efficient modification of all free cysteines in PDI. Subsequently,

NEM was added from a 73 m*M* stock in dimethyl sulfoxide to a final concentration of 20 m*M*, and the mixture was incubated at room temperature for 1 h. At 15 min before this *in vitro* treatment with NEM, the lysate for the reduced control lane (obtained from DTT-treated cells) was additionally supplemented with 10 m*M* TCEP (from a 200 m*M* stock). After immunoprecipitation, proteins were released from the beads by incubation in 50 μl 80 m*M* Tris/HCl, pH 7.0, 2% SDS for 5 min in a heat block at 97°C, followed by vortexing for 5 sec. Then 40 μl of supernatant was transferred to a tube containing 2 μl of 200 m*M* TCEP (~10 mM final concentration) and incubated for 15 min at room temperature to reduce active-site disulfides. Thus, reduced cysteine residues were then alkylated for 1 h at room temperature in 15 m*M* mPEG-mal (15 μl of 55 m*M* stock added and carefully mixed). Excess mPEG-mal was removed by protein precipitation by using methanol/chloroform (see later).

Immunoprecipitation and protein precipitation by methanol/chloroform

After *in vitro* modification with mPEG-mal (single NEM-alkylation variant) or NEM (double NEM-alkylation variant), 850 μl of a buffer containing 30 m*M* triethanolamine, pH 8.1, 100 m*M* NaCl, 5 m*M* EDTA, and 1.5% Triton X-100 was added to the cell lysate, and the mixture was incubated for 30 min on ice before centrifugation in an ultracentrifuge (Beckman Coulter, Fullerton, CA) for 1 h at 100,000 *g* at 4°C. The resulting supernatant was added to 20 μl of protein A-sepharose beads (dry volume) that had been preadsorbed to 2 μl PDI or TMX3 antiserum in 250 μl 100 m*M* $NaHPO_4$/HCl, pH 8.0, 1% Triton X-100 for 2 h under constant agitation at room temperature. Immunoprecipitation was performed for at least 1.5 h on an end-over-end shaker at 4°C. Subsequently, the beads were washed four times in a buffer containing 30 m*M* triethanolamine, pH 8.1, 100 m*M* NaCl, 5 m*M* EDTA, 0.2% SDS, 1% Triton X-100, and once in the same buffer lacking SDS and Triton X-100.

Immunoisolated mPEG-mal–modified PDI or TMX3 obtained after double NEM alkylation was precipitated with methanol/chloroform according to Wessel et al. (35). In brief, one sample volume of methanol was added, followed by vortexing. After the addition of 0.25 sample volumes of chloroform and vortexing, the mixture was centrifuged for 1 min at 20,000 *g* at room temperature for phase separation. The upper phase was discarded, and the protein in the interphase was pelleted after the addition of 0.75 sample volumes of methanol and vortexing by centrifugation for 2 min at 20,000 *g* (all sample volumes compared with the original sample). The supernatant was carefully aspirated, and the pellet dried in a Concentrator 5301 (Eppendorf, Hamburg, Germany) for 15 min at room temperature.

Gel electrophoresis and Western blotting

Washed immunobeads and protein pellets precipitated by methanol/chloroform were supplemented with a suitable volume of 58 m*M* Tris/HCl, pH 6.8, 5% glycerol, 1.67% SDS, 0.002% bromophenol blue, and the proteins were solubilized at 97°C for 5 min. SDS-PAGE was performed in Hoeffer Minigel devices (GE Healthcare) by using 1-mm spacers. Tris-glycine 7.5% polyacrylamide gels (19) of 75-mm length (separating gel) were run at 35 mA until the 50-kDa band of the prestained Dual Color Precision Plus Protein Standard (Biorad, Hercules, CA) reached the bottom of the gel. After electrophoresis, gels were incubated in 40% methanol, 10% acetic acid for 15 min for fixation of polypeptides. Gels were subsequently placed on a piece of wet Whatman paper and dried under vacuum at 80°C for 1 h. Labeled proteins were visualized by scanning on a STORM phosphorimager (GE Healthcare), and quantified by using the ImageQuant Mac v1.2 software (GE Healthcare). Nonradioactive cellular extracts modified with AMS were resolved by SDS-PAGE, transferred by wet blotting, probed with antibodies, and developed as described in (15).

RESULTS

AMS treatment does not resolve oxidized and reduced PDI

In a first attempt to determine the *in vivo* redox state of human PDI, we used the AMS-modification protocol developed earlier [(16), Fig. 1A]. To obtain control samples representing the reduced and oxidized forms of PDI cells were incubated in growth medium supplemented with either 10 m*M* DTT or 5 m*M*

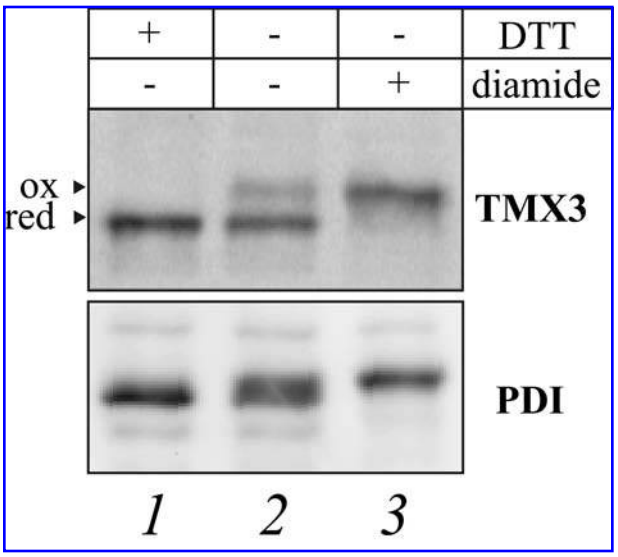

FIG. 2. SDS-PAGE mobility shifts induced by AMS are minimal for PDI. Cell extracts from HEK-293 cells were treated according to the AMS-modification protocol, resolved by SDS-PAGE, and TMX3 (*top panel*) and PDI (*bottom panel*) were visualized with Western blotting by using antisera against the endogenous proteins. Lane 1, reduced control (cells treated with DTT before modification); lane 2, steady-state distribution; lane 3, oxidized control (cells treated with diamide before modification). It was consistently observed that the oxidized form of PDI, unlike that of TMX3, was not well resolved from the reduced form (lane 2, compare the two panels). The same experiment was performed in HeLa, Vero, and CV-1 cells, reliably yielding very similar results (data not shown). Red, reduced form; ox, oxidized form (of TMX3).

diamide. The AMS-modification method, however, consistent with a previous report (5), produced only minimal SDS-PAGE mobility shifts for PDI, whereas a clear separation of the reduced and oxidized forms of the PDI-like ER enzyme TMX3, which contains only a single Cys-Gly-His-Cys active site (15), was readily observed (Fig. 2). Furthermore, simply substituting mPEG-mal for AMS in this protocol was not feasible for technical reasons because of the deleterious effects of mPEG-mal on protein migration by SDS-PAGE and a vastly reduced transfer efficiency from the gel to the membrane during Western blotting (unpublished observation).

Determination of the PDI redox state by mPEG-mal modification

To overcome the disadvantages of these and the previously used methods mentioned in the Introduction, we designed two variants of a procedure involving radioactive labeling and immunoprecipitation (Fig. 3A, lanes 1–3 and lanes 4–6, respectively). An overview of these two procedures in comparison with the AMS-modification method is provided in Fig. 1A. Both protocols eliminated the need for immunoblotting and removed excess mPEG-mal before SDS-PAGE.

In the variant of this protocol that involves only one NEM-alkylation step (Fig. 3A, lanes 1–3), metabolically labeled and NEM-treated HEK-293 cell lysates were first reduced by TCEP. In analogy to the AMS-modification protocol, free sulfhydryl groups appearing as a result of the TCEP treatment were then modified with mPEG-mal ahead of immunoprecipitation of PDI. The result showed a number of bands (lane 2) that collapsed to one major band running at ~55 kDa on reduction of the cells with DTT (lane 1) or ~125 kDa after oxidation with diamide (lane 3). In accordance with the predicted molecular mass of human PDI (55,294 Da), the ~55-kDa species represents nonmodified PDI (0 mPEG-mal; labeled "red"). Unlike Pdi1p that contains a structural disulfide in the **a** domain (36), the two non–active-site cysteines in the **b′** domain of human PDI exist as free thiols (29). Therefore, we assigned the ~125-kDa band (labeled "ox") as PDI modified with four molecules of mPEG-mal, corresponding to oxidation of both active sites as a result of the diamide treatment.

Apart from PDI modified with no and four mPEG-mal molecules, additional bands were detected in lanes 1 and 3. These species appeared as a result of mPEG-mal modification because they did not show in an anti-PDI immunoprecipitation in the absence of the reagent (data not shown). In the oxidized control (lane 3), the mobility of the band at ~150 kDa (labeled with a diamond) corresponded to PDI containing at least five mPEG-mal molecules. Given a 100% efficiency of the *in situ* NEM modification of the two free cysteines in the **b′** domain, only the four active-site cysteines in PDI would expectedly be modified by mPEG-mal after diamide treatment. A likely explanation for the species observed at ~150 kDa in lane 3 was

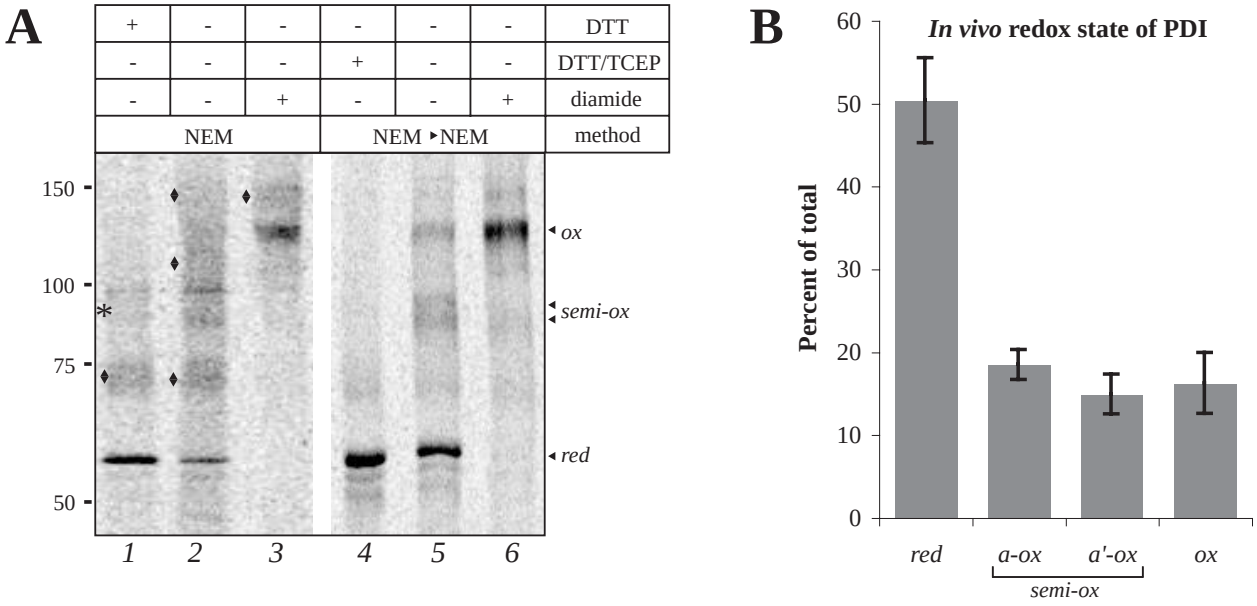

FIG. 3. mPEG-mal based determination of the *in vivo* redox state of PDI requires an improved NEM-alkylation protocol. (**A**) Autoradiogram showing typical results of the single (method, NEM; lanes 1–3) and double (method, NEM ▶ NEM; lanes 4–6) NEM-alkylation protocol performed on PDI in HEK-293 cells. Lanes 1 and 4, reduced control; lanes 2 and 5, steady-state distribution; lanes 3 and 6, oxidized control. In lane 5, the steady-state redox distribution of PDI is visualized by the separation of reduced (red), semioxidized (semi-ox), and fully oxidized (ox) forms of the protein. With the double NEM-alkylation protocol (compare lanes 2 and 5), the modification of a noncatalytic cysteine with mPEG-mal (*diamonds*) is markedly reduced, and no semioxidized PDI (compare lanes 1 and 4, *asterisk*) is observed on TCEP reduction before the *in vitro* NEM-alkylation step (see text for details). The size of molecular mass marker bands is shown on the left. (**B**) Densitometric quantification of the four redox species of PDI (HEK-293 cells, $n = 5$, ±SD). **a**-ox, **a** domain oxidized and **a′** domain reduced; **a′**-ox, **a** domain reduced and **a′** domain oxidized.

therefore inefficient blocking by NEM—and as a result, subsequent mPEG-mal modification—of at least one of the noncatalytic cysteine residues. The same explanation likely accounts for the band in the reduced control at ~70 kDa (lane 1, diamond) and three bands observed at steady-state conditions (lane 2, diamonds). In the recombinant **b′** domain, both cysteines have been found to be quite inaccessible to alkylation by low-molecular-weight thiol-reactive reagents in the native state (29). This finding and the results of the double NEM-alkylation protocol shown in Fig. 3A, lanes 4–6 (see later), gave further support to the interpretation that inefficient *in situ* alkylation by NEM of at least one **b′** cysteine explains the bands labeled by diamonds in Fig. 3.

In addition to the diamond-labeled band at ~70 kDa, we observed a weak band appearing above reduced PDI in lane 1 (asterisk). Because this species co-migrates with semioxidized PDI (see later), it is likely still oxidized in one of the two active sites despite treatment of the cells with DTT. This finding probably reflects the potency of the oxidase Ero1 in catalyzing the oxidation of PDI, even in the face of a reductive challenge caused by DTT (21, 31).

A slightly modified mPEG-mal modification assay (see Fig. 1A) eliminated the caveats described earlier and allowed accurate quantification of the *in vivo* redox state of PDI. To improve the efficiency of NEM modification, the cell lysate was heat denatured and subjected to a second incubation with NEM *in vitro*. Furthermore, in the case of the reduced control (lane 4), TCEP was added to the lysate to completely reduce active-site cysteines before the *in vitro* treatment with NEM, thus increasing the yield of NEM-blocked cysteines ahead of mPEG-mal treatment. Subsequently, the alkylated cell lysates were subjected to anti-PDI immunoprecipitation, thus removing excess NEM. Immunopurified, NEM-modified PDI was then sequentially treated with TCEP and mPEG-mal and precipitated by the methanol/chloroform method ahead of electrophoretic separation and visualization of the reduced and oxidized forms of the protein.

By substantially reducing the signal of the additional bands observed with the single NEM-alkylation variant of the protocol (compare Fig. 3A, lanes 1 + 3 with lanes 4 + 6) this method revealed three clearly separated redox species of PDI at steady state (Fig. 3A, lane 5): fully reduced PDI (red, 0 mPEG-mal), PDI with both active sites (in the **a** and **a′** domains) in the oxidized form (ox, 4 mPEG-mal), and a species of intermediate gel mobility that turned out to represent semioxidized PDI (semi-ox; one active site in the oxidized and the other in the reduced form, 2 mPEG-mal). In the following, we describe the identification of semioxidized PDI.

The species of intermediate gel mobility appeared as a doublet on the phosphorimager scans. Still, both bands showed a gel mobility between reduced and oxidized PDI that could potentially be explained with redox variants of PDI modified with two mPEG-mal molecules. Such species would arise if the active-site cysteines in one redox-active domain were present in the oxidized state, whereas the two active-site cysteines in the other domain would be in the reduced state. Therefore, we transiently transfected HEK-293 cells with cDNAs encoding N-terminally HA-tagged wild-type PDI, and HA-PDI in which the two cysteines in either of the Cys-Gly-His-Cys motifs had been exchanged for Ser and Ala, respectively (Fig. 1C). mPEG-mal–based redox analysis of these cells (Fig. 4) by using an antibody against the HA-epitope for immunoprecipitation showed that indeed these bands denote two semioxidized forms of PDI modified with two molecules of mPEG-mal. The faster-migrating semioxidized species represents PDI modified with mPEG-mal in the **a** domain (**a**-ox, lanes 4 + 7) that can readily be separated from the other semioxidized form (**a′-**ox, lanes 5 + 8).

Having established the molecular identity of the four redox species of PDI present at steady state, we performed a densitometric quantification from five independent experiments. The analysis yielded a steady-state redox distribution of endogenous PDI in HEK-293 cells of 50 ± 5% (SD) fully reduced, 18 ± 2% **a**-oxidized/**a′-**reduced, 15 ± 2% **a**-reduced/**a′**-oxidized, and 16 ± 4% fully oxidized (Fig. 3B). When comparing the results obtained for the endogenous protein with the overexpressed HA-tagged variants, we noticed a couple of slight differences. For unknown reasons, but possibly owing to oversaturation of Ero1 capacity when overexpressing PDI, wild-type HA-PDI consistently appeared less oxidized than endogenous PDI (compare Fig. 4, lane 6, and Fig. 3A, lane 5). Furthermore, overexpressed HA-PDIΔS1 and HA-PDIΔS2 were not completely modified with mPEG-mal on treatment with diamide, as judged by the persistence of a weak band for the reduced form (Fig. 4, lanes 7–8). Finally, it is worth noticing that the minor mobility difference observed between HA-PDI and endogenous (untagged) PDI modified with mPEG-mal (compare the apparent molecular mass of modified forms in Figs. 3 and 4) likely results from the presence of the HA tag on exogenously expressed PDI.

Application of the method to a control protein

Compared with the AMS-modification method, the two protocols involving radioactive labeling and immunoprecipitation comprise a number of additional steps. For instance, an overnight labeling period is required to obtain steady-state information on PDI. Potentially, the cells could suffer from such treatment because only low concentrations of (labeled) methionine and cysteine are available. In turn, this could possibly influence the redox state of the protein under investigation. To test the applicability of the single and double NEM-alkylation protocols for mPEG-mal modification to another protein, in which we already knew the redox distribution from results of the AMS-modification method, we therefore performed both mPEG-mal modification procedures on TMX3.

Both the single and the double NEM-alkylation variants produced a clear visualization of reduced and oxidized TMX3 (Fig. 5). Three background bands were co-precipitated with anti-TMX3 (asterisks), and one mPEG-mal–dependent band was observed at ~100 kDa (double asterisk). *A priori*, the latter band could be related to TMX3 that contains two noncatalytic cysteines in the transmembrane region in addition to the two active-site cysteines (15). However, the fact that the appearance of this band is unchanged between the DTT and diamide lanes (*i.e.*, it does not co-shift with the TMX3 band on modification in the active site) indicates that it is likely also unrelated to

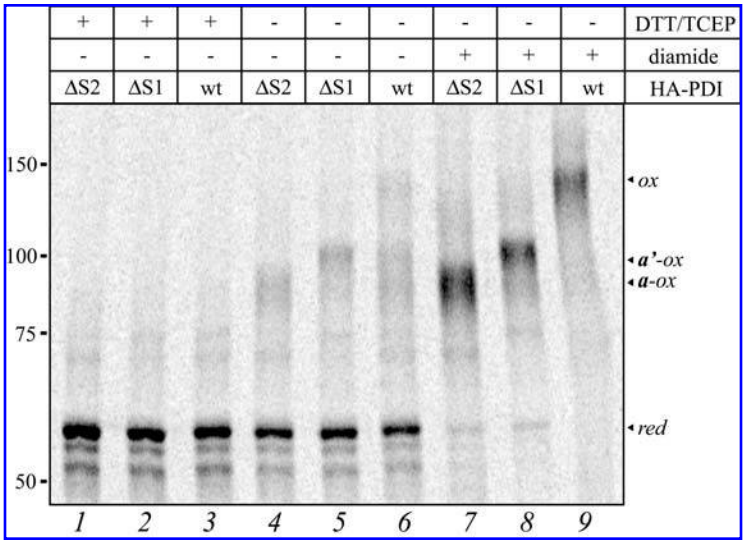

FIG. 4. The two semioxidized forms of PDI can be differentiated by modification with mPEG-mal. HEK-293 cells were transfected with pcDNA3/HA-PDI (wt), pcDNA3/HA-PDIΔS1 (ΔS1), and pcDNA3/HA-PDIΔS2 (ΔS2) cDNA, and subjected to the double NEM-alkylation protocol followed by immunoprecipitation using an anti-HA antibody and by modification with mPEG-mal. Reduced (DTT/TCEP) (lanes 1–3) and oxidized (diamide) (lanes 7–9) control samples were obtained, as detailed in the text. PDI redox species are labeled as in Fig. 3B.

TMX3. As can be seen when comparing Fig. 2, lane 2, with Fig. 5, lanes 2 and 5, the results were in mutual agreement, with redox ratios of ~70% reduced and ~30% oxidized TMX3, irrespective of the method used. As judged by this experiment, the methods requiring radioactive labeling and immunoprecipitation did therefore not appear inadvertently to introduce any biasing of the results.

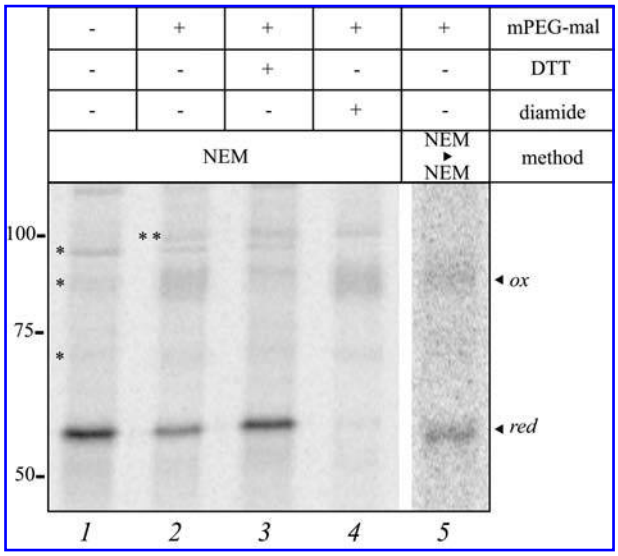

FIG. 5. Single and double NEM-alkylation protocols are equivalent in trapping the redox state of TMX3. Shown are the results of two independent experiments using either the single (method, NEM) or double (method, NEM ▶ NEM) NEM-alkylation protocol performed on TMX3 in HEK-293 cells. Reduced (lane 3) and oxidized (lane 4) controls are shown for the single NEM-alkylation experiment only, but were the same in the double NEM-alkylation experiment. Note that one of the background bands (*asterisks*) coalesces with the oxidized form (ox). Molecular mass markers are indicated. *Double asterisk*, mPEG-mal-dependent background band; red, reduced form.

DISCUSSION

We have shown here that the sequential modification of NEM-treated, immunoisolated, and radioactively labeled endogenous human PDI with TCEP and mPEG-mal provides a quantitative and highly reproducible readout that clearly discriminates between the reduced and the oxidized states of the protein. With ~50% totally reduced PDI observed here, the human enzyme is apparently less oxidized than Pdi1p in living yeast cells, where only ~30% is in the totally reduced form (13, 37). Recent work performed *in vitro* on Pdi1p indicated that also semioxidized forms of the enzyme would potentially exist in living cells (18). Thus, it was shown that in the full-length protein, the **a′** domain of Pdi1p is oxidized faster by Ero1 than the **a** domain. In addition, Ero1-mediated oxidation of the latter domain was inhibited in the presence of substrate. In another study, a semioxidized form of Pdi1p was trapped *in vivo*, but its molecular identification was not pursued (37). The present work for the first time visualizes the presence and quantifies the levels of two molecularly defined semioxidized forms of PDI *in vivo*. This finding—exemplified here for human PDI—likely also applies to other PDI orthologues.

Our results will now allow detailed *in vivo* investigations of the two separate active sites in PDI. Such studies should have interesting biological implications. For instance, as changes in the *in vivo* redox state of PDI on overexpression or mutation of Ero1 are well established (13, 21), it will be particularly interesting to learn whether—and if so, how—these sites are differentially regulated *in vivo* by the two human isoforms of Ero1, Ero1α and β (4, 26). Under the normal cellular conditions investigated here, we observed no significant difference in the levels of the two semioxidized forms. However, it will now be possible to examine the redox state of PDI in living cells during conditions in which the ER environment is perturbed, for instance, on accumulation of misfolded proteins in which PDI is known to play a role in facilitating the retrotranslocation of substrates for ER-associated degradation to the cytosol (12). Likewise, the present technique may prove helpful when studying posttranslational modification of redox-active cysteines un-

der cellular stress conditions, such as nitrosative stress that is known to S-nitrosylate active-site cysteines in PDI (34). Overall, this assay—when applied not only to PDI but also to other redox-active ER enzymes in combination with various means to perturb ER redox homeostasis—will help decipher the redox pathways in the ER of mammalian cells in a more quantitative manner than previously possible.

PDI and its homologues catalyze reduction, oxidation, and isomerization by disulfide exchange that proceeds through a transient mixed disulfide between enzyme and substrate. Reoxidation of PDI by Ero1 occurs by the same type of reaction. Still, regardless of the method—acid trapping or NEM treatment—used to block free cysteines, it has proven difficult to visualize transient mixed-disulfide complexes in mammalian tissue-culture cells. Even when host protein synthesis is blocked by virus infection and the ER is loaded with viral glycoproteins that are substrates of PDI and its closest homologue, ERp57, mixed-disulfide complexes between these enzymes and their substrates are still not straightforward to visualize (22). Currently, only two examples of trapped mixed-disulfide complexes of PDI with an endogenous substrate in mammalian cells are known. Ahn and colleagues (28) recently reported a disulfide intermediate between PDI and MHC class I heavy chain in NEM-treated HeLa cells, in which analysis of 5×10^8 cells was needed for detection. Visualization of mixed-disulfide complexes of PDI (and ERp57) with the highly expressed thyroglobulin, a slowly maturing protein containing 60 disulfides, in NEM-treated thyrocytes required less cell material (8). In addition, mixed-disulfides between PDI and Ero1 have been documented both in yeast and in human cells (2, 13, 21).

Why is it so difficult to trap mixed-disulfide complexes of PDI family members and their substrates? The predominant reason is likely the transient nature of the complex. Whereas reduction and oxidation reactions are intrinsically fast, intramolecular isomerization would be slower. However, *in vitro* experiments suggest that cycles of reduction and oxidation constitute the predominant reaction mechanism for isomerization (30). Therefore, complexes in the process of intramolecular isomerization are likely rare, reducing the probability of trapping even these slower-reacting species.

Still, with acid-trapping, Gilbert and colleagues (37) recently reported mPEG-mal–modified forms of Pdi1p that showed gel mobilities consistent with odd numbers of mPEG-mal molecules attached to their active sites. These species may potentially represent Pdi1p in mixed-disulfide complexes with other proteins or with glutathione. Alternatively, they could arise because of difficulties in modifying two cysteines within the same active site with the quite large mPEG-mal molecule, an explanation previously used to rationalize similar species found when modifying purified, trichloroacetic acid–precipitated PDI with mPEG-mal (30). The *in situ* NEM-alkylation protocol used here efficiently blocks active-site cysteines of various PDI-like enzymes when present in the dithiol form, as for instance seen for TMX3 (Fig. 2, lane 1, and our unpublished observations). Likewise, the experimental setup with heat denaturation in a buffer containing SDS ahead of incubation with mPEG-mal ensures complete modification of both active-site cysteines with mPEG-mal. By using these conditions, we observed no forms of human PDI that were modified with an odd number of mPEG-mal molecules in the active sites, a finding that would have been indicative of mixed-disulfide complexes. Although this is likely due to their transient nature, at present we cannot rule out that steric hindrance may result in inefficient blocking by NEM of the C-terminal active-site cysteine in a putative mixed-disulfide complex (involving the N-terminal active site cysteine). During cell homogenization, the complex would then dissociate because of nucleophilic attack by the free C-terminal cysteine, resulting in oxidation of the active site. Therefore, a fraction of the semioxidized and oxidized forms of PDI reported here could represent PDI originally present in mixed-disulfide complexes.

The increased resolution of our method as compared with the modest AMS-induced shift observed for PDI (see Fig. 2) relies on the substantially larger molecular mass of mPEG-mal as compared with AMS. Contrary to PDI, we observed a significant AMS-induced mobility shift for TMX3, even though this protein contains only a single Cys-Gly-His-Cys active site (see Fig. 2). Similarly, we noticed that modification of other PDI-like proteins by the AMS method rarely results in shifts that correlate directly with the number of active-site sequence motifs (unpublished observation). Here, we also observed a difference in gel migration of the two semioxidized forms of PDI that are both modified with two molecules of mPEG-mal. The reason behind these observations is currently unclear. It is worth noting that because mPEG-mal binds water, the observed mobility shift induced by the attachment of one mPEG-mal molecule by far exceeds its actual molecular mass of 5 kDa, as also noticed previously (3, 14, 17, 30, 33, 37).

The determination of the redox state of PDI required the use of the double NEM-alkylation variant of the protocol. However, redox analysis of TMX3 was readily performed by using the more simple single NEM-alkylation protocol. Similarly, this variant of the procedure will likely be able to establish the oxidation status of most other proteins *in vivo*. In particular, this method should prove useful for large proteins with only one or few structural disulfides, in which detection by SDS-PAGE mobility shifts based on the oxidation status of the protein is most often not feasible. Most evidence for the presence of disulfides in such proteins is indirect, obtained either from mutational analysis of cysteine residues, or from sensitivity toward reducing or thiol-modifying agents such as DTT and NEM, respectively (see for instance refs. 6, 10, 11, and 38). A prominent example of proteins in this category is G protein–coupled receptors. In this very large family of proteins, most contain two conserved cysteines in adjacent extracellular loops proposed to form a disulfide bond, which is in many cases crucial for the function of the protein. Direct evidence for the existence of this disulfide throughout the entire family is scarce, and primarily comes from the crystal structure of rhodopsin (27) and from *in vitro* work performed on recombinantly expressed and purified protein such as the leukotriene B_4 receptor (1). The mPEG-mal method described here should provide a direct means to establish the *in vivo* oxidation state of these important proteins.

ACKNOWLEDGMENTS

We thank Christel Elkjær Olsen and Jan Riemer for help with cDNA cloning, Sandra Abel Nielsen for excellent technical as-

sistance, the Institute of Biochemistry, ETH Zürich, for the continued support, and Roberto Sitia (Milan) and Jakob R. Winther (Copenhagen) for cDNA constructs. We also thank all members of the Ellgaard laboratory and Jacob R. Winther for critical reading of the manuscript. Funding obtained from the Swiss National Science Foundation, the Novartis Stiftung, Carlsbergfondet, A. P. Møllers Fond til Lægevidenskabens Fremme and Novo Nordisk Fonden is gratefully acknowledged.

ABBREVIATIONS

AMS, 4-acetamido-4′-maleimidylstilbene-2,2′-disulfonic acid; DTT, dithiothreitol; ER, endoplasmic reticulum; Ero1, ER oxidase 1; mPEG-mal, methoxy polyethylene glycol 5000 maleimide; NEM, *N*-ethylmaleimide; PBS, phosphate-buffered saline; PDI, protein disulfide isomerase; PMSF, phenylmethylsulfonylfluoride; redox, reduction–oxidation; Pdi1p, *S. cerevisiae* PDI; TCEP, Tris(2-carboxyethyl)phosphine; TMX3, thioredoxin-related transmembrane protein 3.

REFERENCES

1. Baneres JL, Martin A, Hullot P, Girard JP, Rossi JC, and Parello J. Structure-based analysis of GPCR function: conformational adaptation of both agonist and receptor upon leukotriene B4 binding to recombinant BLT1. *J Mol Biol* 329: 801–814, 2003.
2. Benham AM, Cabibbo A, Fassio A, Bulleid N, Sitia R, and Braakman I. The CXXCXXC motif determines the folding, structure and stability of human Ero1-Lalpha. *EMBO J* 19: 4493–4502, 2000.
3. Bjornberg O, Ostergaard H, and Winther JR. Mechanistic insight provided by glutaredoxin within a fusion to redox-sensitive yellow fluorescent protein. *Biochemistry* 45: 2362–2371, 2006.
4. Cabibbo A, Pagani M, Fabbri M, Rocchi M, Farmery MR, Bulleid NJ, and Sitia R. ERO1-L, a human protein that favors disulfide bond formation in the endoplasmic reticulum. *J Biol Chem* 275: 4827–4833, 2000.
5. Chakravarthi S and Bulleid NJ. Glutathione is required to regulate the formation of native disulfide bonds within proteins entering the secretory pathway. *J Biol Chem* 279: 39872–39879, 2004.
6. D'Angelo DD, Eubank JJ, Davis MG, and Dorn GW 2nd. Mutagenic analysis of platelet thromboxane receptor cysteines: roles in ligand binding and receptor-effector coupling. *J Biol Chem* 271: 6233–6240, 1996.
7. Darby NJ, Penka E, and Vincentelli R. The multi-domain structure of protein disulfide isomerase is essential for high catalytic efficiency. *J Mol Biol* 276: 239–247, 1998.
8. Di Jeso B, Park YN, Ulianich L, Treglia AS, Urbanas ML, High S, and Arvan P. Mixed-disulfide folding intermediates between thyroglobulin and endoplasmic reticulum resident oxidoreductases ERp57 and protein disulfide isomerase. *Mol Cell Biol* 25: 9793–9805, 2005.
9. Ellgaard L and Ruddock LW. The human protein disulphide isomerase family: substrate interactions and functional properties. *EMBO Rep* 6: 28–32, 2005.
10. Elliott C, Muller J, Miklis M, Bhat RA, Schulze-Lefert P, and Panstruga R. Conserved extracellular cysteine residues and cytoplasmic loop-loop interplay are required for functionality of the heptahelical MLO protein. *Biochem J* 385: 243–254, 2005.
11. Flahaut M, Pfister C, Rossier BC, and Firsov D. N-Glycosylation and conserved cysteine residues in RAMP3 play a critical role for the functional expression of CRLR/RAMP3 adrenomedullin receptor. *Biochemistry* 42: 10333–10341, 2003.
12. Forster ML, Sivick K, Park YN, Arvan P, Lencer WI, and Tsai B. Protein disulfide isomerase-like proteins play opposing roles during retrotranslocation. *J Cell Biol* 173: 853–859, 2006.
13. Frand AR and Kaiser CA. Ero1p oxidizes protein disulfide isomerase in a pathway for disulfide bond formation in the endoplasmic reticulum. *Mol Cell* 4: 469–477, 1999.
14. Guo ZY, Chang CC, Lu X, Chen J, Li BL, and Chang TY. The disulfide linkage and the free sulfhydryl accessibility of acyl-coenzyme A: cholesterol acyltransferase 1 as studied by using mPEG5000-maleimide. *Biochemistry* 44: 6537–6546, 2005.
15. Haugstetter J, Blicher T, and Ellgaard L. Identification and characterization of a novel thioredoxin-related transmembrane protein of the endoplasmic reticulum. *J Biol Chem* 280: 8371–8380, 2005.
16. Jessop CE and Bulleid NJ. Glutathione directly reduces an oxidoreductase in the endoplasmic reticulum of mammalian cells. *J Biol Chem* 279: 55341–55247, 2004.
17. Katzen F and Beckwith J. Role and location of the unusual redox-active cysteines in the hydrophobic domain of the transmembrane electron transporter DsbD. *Proc Natl Acad Sci U S A* 100: 10471–10476, 2003.
18. Kulp MS, Frickel EM, Ellgaard L, and Weissman JS. Domain architecture of protein-disulfide isomerase facilitates its dual role as an oxidase and an isomerase in Ero1p-mediated disulfide formation. *J Biol Chem* 281: 876–884, 2006.
19. Laemmli UK. Cleavage of structural proteins during the assembly of the head of bacteriophage T4. *Nature* 227: 680–685, 1970.
20. Lumb RA and Bulleid NJ. Is protein disulfide isomerase a redox-dependent molecular chaperone? *EMBO J* 21: 6763–6770, 2002.
21. Mezghrani A, Fassio A, Benham A, Simmen T, Braakman I, and Sitia R. Manipulation of oxidative protein folding and PDI redox state in mammalian cells. *EMBO J* 20: 6288–6296, 2001.
22. Molinari M and Helenius A. Glycoproteins form mixed disulphides with oxidoreductases during folding in living cells. *Nature* 402: 90–93, 1999.
23. Molteni SN, Fassio A, Ciriolo MR, Filomeni G, Pasqualetto E, Fagioli C, and Sitia R. Glutathione limits Ero1-dependent oxidation in the endoplasmic reticulum. *J Biol Chem* 279: 32667–32673, 2004.
24. Nardai G, Stadler K, Papp E, Korcsmaros T, Jakus J, and Csermely P. Diabetic changes in the redox status of the microsomal protein folding machinery. *Biochem Biophys Res Commun* 334: 787–795, 2005.
25. Otsu M, Bertoli G, Fagioli C, Guerini-Rocco E, Nerini-Molteni S, Ruffato E, and Sitia R. Dynamic retention of Ero1alpha and Ero1beta in the endoplasmic reticulum by interactions with PDI and ERp44. *Antioxid Redox Signal* 8: 274–282, 2006.
26. Pagani M, Fabbri M, Benedetti C, Fassio A, Pilati S, Bulleid NJ, Cabibbo A, and Sitia R. Endoplasmic reticulum oxidoreductin 1-lbeta (ERO1-Lbeta), a human gene induced in the course of the unfolded protein response. *J Biol Chem* 275: 23685–23692, 2000.
27. Palczewski K, Kumasaka T, Hori T, Behnke CA, Motoshima H, Fox BA, Le Trong I, Teller DC, Okada T, Stenkamp RE, Yamamoto M, and Miyano M. Crystal structure of rhodopsin: a G protein-coupled receptor. *Science* 289: 739–745, 2000.
28. Park B, Lee S, Kim E, Cho K, Riddell SR, Cho S, and Ahn K. Redox regulation facilitates optimal peptide selection by MHC class I during antigen processing. *Cell* 127: 369–382, 2006.
29. Pirneskoski A, Klappa P, Lobell M, Williamson RA, Byrne L, Alanen HI, Salo KE, Kivirikko KI, Freedman RB, and Ruddock LW. Molecular characterization of the principal substrate binding site of the ubiquitous folding catalyst protein disulfide isomerase. *J Biol Chem* 279: 10374–10381, 2004.
30. Schwaller M, Wilkinson B, and Gilbert HF. Reduction-reoxidation cycles contribute to catalysis of disulfide isomerization by protein-disulfide isomerase. *J Biol Chem* 278: 7154–7159, 2003.
31. Sevier CS, Qu H, Heldman N, Gross E, Fass D, and Kaiser CA. Modulation of cellular disulfide-bond formation and the ER redox environment by feedback regulation of Ero1. *Cell* 129: 333–344, 2007.
32. Tian G, Xiang S, Noiva R, Lennarz WJ, and Schindelin H. The crystal structure of yeast protein disulfide isomerase suggests cooperativity between its active sites. *Cell* 124: 61–73, 2006.
33. Tsai B and Rapoport TA. Unfolded cholera toxin is transferred to the ER membrane and released from protein disulfide isomerase upon oxidation by Ero1. *J Cell Biol* 159: 207–216, 2002.

34. Uehara T. Accumulation of misfolded protein through nitrosative stress linked to neurodegenerative disorders. *Antioxid Redox Signal* 9: 597–601, 2007.
35. Wessel D and Flugge UI. A method for the quantitative recovery of protein in dilute solution in the presence of detergents and lipids. *Anal Biochem* 138: 141–143, 1984.
36. Wilkinson B, Xiao R, and Gilbert HF. A structural disulfide of yeast protein-disulfide isomerase destabilizes the active site disulfide of the N-terminal thioredoxin domain. *J Biol Chem* 280: 11483–11487, 2005.
37. Xiao R, Wilkinson B, Solovyov A, Winther JR, Holmgren A, Lundstrom-Ljung J, and Gilbert HF. The contributions of protein disulfide isomerase and its homologues to oxidative protein folding in the yeast endoplasmic reticulum. *J Biol Chem* 279: 49780–49786, 2004.
38. Zhang P, Johnson PS, Zollner C, Wang W, Wang Z, Montes AE, Seidleck BK, Blaschak CJ, and Surratt CK. Mutation of human mu opioid receptor extracellular "disulfide cysteine" residues alters ligand binding but does not prevent receptor targeting to the cell plasma membrane. *Brain Res Mol Brain Res* 72: 195–204, 1999.

Address reprint requests to:
Lars Ellgaard
Department of Molecular Biology
University of Copenhagen
August Krogh Building
Universitetsparken 13
2100 Copenhagen Ø, Denmark

E-mail: lellgaard@aki.ku.dk

Date of first submission to ARS Central, July 17, 2007; date of acceptance, August 10, 2007.

This article has been cited by:

1. Randi H. Gottfredsen, Sophie My-Hang Tran, Ulrike G. Larsen, Peder Madsen, Morten S. Nielsen, Jan J. Enghild, Steen V. Petersen. 2012. The C-terminal proteolytic processing of extracellular superoxide dismutase is redox regulated. *Free Radical Biology and Medicine* **52**:1, 191-197. [CrossRef]
2. Rossella Sgarbanti , Lucia Nencioni , Donatella Amatore , Paolo Coluccio , Alessandra Fraternale , Patrizio Sale , Caterina L. Mammola , Guido Carpino , Eugenio Gaudio , Mauro Magnani , Maria R. Ciriolo , Enrico Garaci , Anna Teresa Palamara . 2011. Redox Regulation of the Influenza Hemagglutinin Maturation Process: A New Cell-Mediated Strategy for Anti-Influenza Therapy. *Antioxidants & Redox Signaling* **15**:3, 593-606. [Abstract] [Full Text HTML] [Full Text PDF] [Full Text PDF with Links]
3. Lori A Rutkevich, David B Williams. 2011. Participation of lectin chaperones and thiol oxidoreductases in protein folding within the endoplasmic reticulum. *Current Opinion in Cell Biology* **23**:2, 157-166. [CrossRef]
4. Christian Appenzeller-Herzog, Jan Riemer, Ester Zito, King-Tung Chin, David Ron, Martin Spiess, Lars Ellgaard. 2010. Disulphide production by Ero1#–PDI relay is rapid and effectively regulated. *The EMBO Journal* **29**:19, 3318-3329. [CrossRef]
5. Pekka Määttänen, Kalle Gehring, John J.M. Bergeron, David Y. Thomas. 2010. Protein quality control in the ER: The recognition of misfolded proteins. *Seminars in Cell & Developmental Biology* **21**:5, 500-511. [CrossRef]
6. Doris Roth, Emily Lynes, Jan Riemer, Henning G. Hansen, Nils Althaus, Thomas Simmen, Lars Ellgaard. 2010. A di-arginine motif contributes to the ER localization of the type I transmembrane ER oxidoreductase TMX4. *Biochemical Journal* **425**:1, 195-205. [CrossRef]
7. Hadas Peled-Zehavi , Shira Avital , Avihai Danon Methods of Redox Signaling by Plant Thioredoxins 251-256. [Abstract] [Summary] [Full Text PDF] [Full Text PDF with Links]
8. Feras Hatahet , Lloyd W. Ruddock . 2009. Protein Disulfide Isomerase: A Critical Evaluation of Its Function in Disulfide Bond Formation. *Antioxidants & Redox Signaling* **11**:11, 2807-2850. [Abstract] [Full Text HTML] [Full Text PDF] [Full Text PDF with Links]
9. Rosa E. Hansen, Jakob R. Winther. 2009. An introduction to methods for analyzing thiols and disulfides: Reactions, reagents, and practical considerations. *Analytical Biochemistry* **394**:2, 147-158. [CrossRef]
10. Yuichiro Shimizu , Linda M. Hendershot . 2009. Oxidative Folding: Cellular Strategies for Dealing with the Resultant Equimolar Production of Reactive Oxygen Species. *Antioxidants & Redox Signaling* **11**:9, 2317-2331. [Abstract] [Full Text HTML] [Full Text PDF] [Full Text PDF with Links]
11. Hiroshi Kadokura, Jon Beckwith. 2009. Detecting Folding Intermediates of a Protein as It Passes through the Bacterial Translocation Channel. *Cell* **138**:6, 1164-1173. [CrossRef]
12. Watson J Lees. 2008. Small-molecule catalysts of oxidative protein folding. *Current Opinion in Chemical Biology* **12**:6, 740-745. [CrossRef]
13. Karl M Baker, Seema Chakravarthi, Kevin P Langton, Alyson M Sheppard, Hui Lu, Neil J Bulleid. 2008. Low reduction potential of Ero1# regulatory disulphides ensures tight control of substrate oxidation. *The EMBO Journal* **27**:22, 2988-2997. [CrossRef]
14. Christian Appenzeller-Herzog, Jan Riemer, Brian Christensen, Esben S Sørensen, Lars Ellgaard. 2008. A novel disulphide switch mechanism in Ero1# balances ER oxidation in human cells. *The EMBO Journal* **27**:22, 2977-2987. [CrossRef]
15. Salvador Ventura . 2008. Oxidative Protein Folding: From the Test Tube to In Vivo Insights. *Antioxidants & Redox Signaling* **10**:1, 51-54. [Citation] [Full Text PDF] [Full Text PDF with Links]
16. Dipak K. Das Methods in Redox Signaling . [Citation] [Full Text HTML] [Full Text PDF] [Full Text PDF with Links]